RESEARCH ARTICLE

Determination of the 5d6p ^{3}F$_4$–5d^2 ^{3}F transition probabilities of Ba I

Jia-qi ZHONG (仲嘉琪)[1,2,3,*], **Geng-hua YU** (余庚华)[1,2,3], **Jin WANG** (王谨)[1,2],

Ming-sheng ZHAN (詹明生)[1,2,†]

[1] *State Key Laboratory of Magnetic Resonance and Atomic and Molecular Physics,*

Wuhan Institute of Physics and Mathematics, Chinese Academy of Sciences, Wuhan 430071, China

[2] *Center for Cold Atom Physics, Chinese Academy of Sciences, Wuhan 430071, China*

[3] *Graduate University of the Chinese Academy of Sciences, Beijing 100049, China*

*E-mail: *jqzhong@wipm.ac.cn, †mszhan@wipm.ac.cn*

Whether the transitions between 6s5d ^{3}D and 5d6p ^{3}F can be used for laser cooling of barium heavily depends upon the transition probabilities of 5d6p ^{3}F–5d^2 ^{3}F. Taking the transition 6s5d ^{3}D$_3$–5d6p ^{3}F$_4$ as a scale, the leakage rate of 5d6p ^{3}F$_4$–5d^2 ^{3}F was used to evaluate the transition probabilities. 706 nm laser pulses with different durations were applied to a barium atomic beam for 6s5d ^{3}D$_3$–5d^2 ^{3}F$_4$ optical pumping, and the remaining percentages in 6s5d ^{3}D$_3$ were measured. After exponential fitting, the transition probability of 5d6p ^{3}F$_4$–5d^2 ^{3}F$_{3,4}$ was determined to be $2.1(4)\times10^4$ s^{-1}, which is in agreement with theoretical calculations using the scaled Thomas–Fermi–Dirac method.

Keywords laser cooling, leakage rate, transition probability, scaled Thomas–Fermi–Dirac method

PACS numbers 37.10.De, 37.10.Jk, 32.70.Cs, 31.15.bt

1 Introduction

Laser cooling and trapping has already been achieved in many alkaline-earth neutral atoms, and the stability of optical frequency standard based on these trapped atoms (e.g. Sr) have reached a very high level [1]. However, because of its complicated energy structure, laser cooling and trapping of barium was not realized until 2008 [2]. In Willman's group at the University of Groningen (Netherlands), three cooling and five trapping lasers of different frequencies were used. Since the 6s5d ^{3}D states were estimated to have long lifetimes [3] and easily populated, the 6s5d ^{3}D–5d6p ^{3}F transitions will possibly be expected to be part of a simpler and more effective scheme for barium cooling and trapping. Also, the ultra-narrow linewidth of the 6s5d ^{3}D$_2$–6s^2 ^{1}S$_0$ transition makes barium a promising candidate for a new active atomic clock.

Especially for the 6s5d ^{3}D$_3$–5d6p ^{3}F$_4$ transition, due to selection rules, the atoms in 5d6p ^{3}F$_4$ cannot decay into other fine levels of 6s5d ^{3}D states except ^{3}D$_3$, and the 5d6p ^{3}F$_4$–6s5d ^{1}D$_2$ transition is also forbidden, so the only theoretically possible leaking channel is 5d6p ^{3}F$_4$–5d^2 ^{3}F$_{3,4}$. However, because the energy level spacing

between 5d6p ^{3}F and 5d^2 ^{3}F is very small, the transition probabilities were expected to be rather small. As can be estimated, if the branching ratio of 5d6p ^{3}F$_4$–5d^2 ^{3}F$_{3,4}$ were less than 10^{-5}, the transition 6s5d ^{3}D$_3$–5d6p ^{3}F$_4$ could be considered to be quasi-closed, and laser cooling and trapping of barium could be realized by a single 706 nm laser. The transition probability of 6s5d ^{3}D$_3$–5d6p ^{3}F$_4$ was experimentally determined to be 5.0×10^7 s^{-1} [4]. However, at present, there is no experimental data available about the transition probabilities of 5d6p ^{3}F–5d^2 ^{3}F.

It is difficult to measure the transition probabilities of 5d6p ^{3}F–5d^2 ^{3}F directly because of the long wavelength and the weakness of the transition. Therefore, since 5d6p ^{3}F$_4$–5d^2 ^{3}F$_{3,4}$ is the only leaking channel of the 6s5d ^{3}D$_3$–5d6p ^{3}F$_4$ transition, we carried out a measurement of the 5d6p ^{3}F$_4$–5d^2 ^{3}F$_{3,4}$ transition indirectly by measuring the leakage rate of the 6s5d ^{3}D$_3$–5d6p ^{3}F$_4$ transition. We applied a counter-propagating 706 nm laser pulse to the atomic beam where the atoms had been populated to 6s5d ^{3}D$_3$. The number of the 6s5d ^{3}D$_3$–5d6p ^{3}F$_4$ transition cycles was adjusted by varying the duration of the pulse, and the remaining percentages of the atoms in ^{3}D$_3$ represented by the relative intensity of

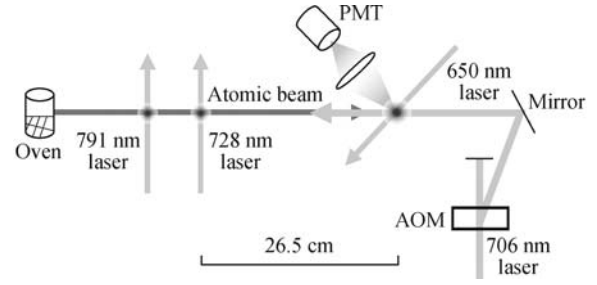the fluorescence were finally recorded.

Before the experiment, the scaled Thomas–Fermi–Dirac (STFD) method [5] was used to theoretically calculate the transition probabilities of 5d6p ^{3}F–5d^2 ^{3}F. In the following section, the results are listed and compared with our experimental data.

2 Experimental measurement

The low lying fine structure and transitions of barium about this work are shown in Fig. 1, and the schematic experimental setup is shown in Fig. 2. A barium beam was produced by a resistively heated oven at 1070(20) K. After leaving the oven, the atoms were perpendicularly excited by a 791.35 nm laser beam and a following 728.23 nm laser beam with the diameters 5 mm for both and the optical power 7 mW and 6 mW respectively. During the first interaction with the 791 nm laser, the atoms were excited to the 6s6p ^{3}P$_1$ state and spontaneously decayed to longlife metastable states 6s5d ^{3}D$_1$ and ^{3}D$_2$. Subsequently, the atoms in 6s5d ^{3}D$_2$ were optically pumped to the 6s5d ^{3}D$_3$ state through the 728 nm stimulated transition. After two steps of optical pumping, about 40% atoms had reached 6s5d ^{3}D$_3$ state. Another counter-propagating pulsed 706.19 nm laser resonant with the 6s5d ^{3}D$_3$–5d6p ^{3}F$_4$ transition was switched by an acousto–optical modulator (AOM) and imposed on the atomic beam to drive the transition cycles. The laser was with the power 5 mW and the beam was slightly focused toward the oven orifice. At the end of the setup, to detect the number of the atoms in 6s5d ^{3}D$_3$, a 650.06 nm probe laser, with the optical power 1 mW and the beam diameter 5 mm, crossed the atomic beam at a angle of 45°. The atoms were excited to 5d6p ^{3}D$_3$, and the fluorescence during the spontaneous radiation was collected and focused to a photomultiplier tube (PMT).
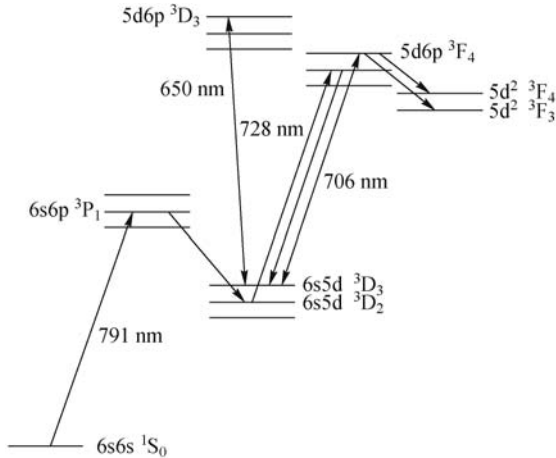
Fig. 2 The experimental layout geometry. After leaving the oven, the barium atoms were successively excited by 791 nm, 728 nm laser perpendicularly, and 650 nm laser at an angle of 45°. Another AOM-switched 706 nm laser was counter-propagating with the atomic beam and the fluorescence from the third cross was collected to a PMT.

The time-varying fluorescence signals corresponding to 100 μs and 400 μs 706 nm laser pulses are shown in Fig. 3. as examples. The horizontal axis represents the time zeroed at the starting point of the pulse, the durations of the pulses are also shown. The vertical axis shows the intensity of the fluorescence in arbitrary units. As can be seen from the curves, the intensity of the fluorescence decreased over time, reached a minimum, and recovered. Because of the Doppler effect, the atoms excited by the counter-propagating laser had almost the same velocities, therefore the horizontal coordinates also represent the relative spatial position of atoms which interacted with the laser for different time spans. In this experiment, the minimum value of the curves decreased when the duration of the pulse increased. However, the minimum did not continue to decrease when the duration was longer than about 350 μs, and the minimum fluorescence intensity for 400 μs was equal to the level caused by the CW laser. Since the Doppler shift caused by the cooling effect in such a short time was much smaller than the natural line width, for durations longer than 400 μs or CW, all of the atoms resonant with the 706 nm laser were optically pumped to the 5d^2 ^{3}F states finally. The
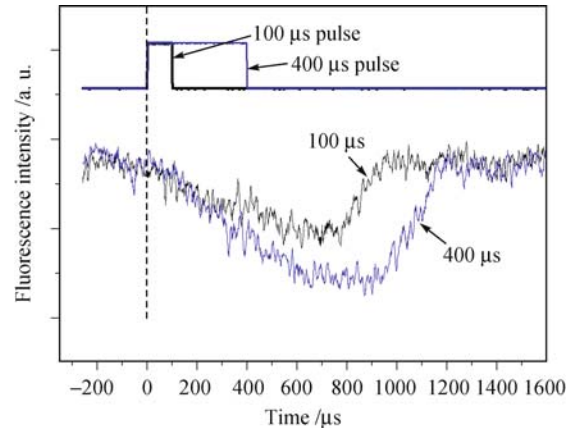

Fig. 1 The diagram of low lying energy levels and transitions of Ba I about this work. The 791 nm transition and 728 nm transition are for the two-step optical pumping, the 706 nm transition for circular excitation, and the 650 nm transition for the population probing of 6s5d ^{3}D$_3$.

Fig. 3 The time-varying fluorescence signal for 100 μs and 400 μs 706 nm laser pulse. Longer duration of the laser pulse corresponds to less population of the remaining atoms in 6s5d ^{3}D$_3$. The durations of the laser pulses are also shown at the top to represent that the horizontal axis is zeroed at the starting point of the 706 nm laser pulse.

diameter of the 706 nm laser was a little smaller than that of the 650 nm probe laser and the atomic beam at the probing region, which made the intensity of the fluorescence stop decreasing to absolute zero. The power broadening of the 650 nm probe laser, which made the atoms with adjacent velocities also excited when probing, was another important reason. Accordingly, the CW background would not affect our measurement and data analysis.

According to the measurement of Garcia [4], the transition probability of 6s5d $^3D_3$–5d6p $^3F_4$ is 5.0×10^7 s^{-1}. Given the intensity of the pumping laser, we can calculate the average number of transition cycles that the atoms experienced during the laser pulse,

$$n = \Delta t A_{ik} \cdot \frac{I/I_s}{1 + I/I_s} \tag{1}$$

where Δt is the duration of the laser pulse, A_{ik} is the transition probability between the lower and the upper energy levels, I is the intensity of the laser field and I_s is the saturation intensity. For the transition 6s5d $^3D_3$–5d6p $^3F_4$, A_{ik} is 5.0×10^7 s^{-1}, I_s is 2.95 mW/cm^2, and the typical I of 706 nm laser is about 50 times of the I_s. We tried different durations of the laser pulse, and the percentage of the remaining atoms in 6s5d $^3D_3$ were recorded. Theoretically, the percentage has exponential relation to the cycling times, where the base of the exponent is the difference between 1 and the leakage rate. The data, plotted in Fig. 4. was fitted with the exponent function,

$$x/\% = (1 - a)^n \tag{2}$$

where n is the number of transition cycles and a is the leakage rate to 5d^2 ^3F. Finally, we find a=4.1E-4 with the fitting error 1E-5 and the averaged random standard error 8E-5.
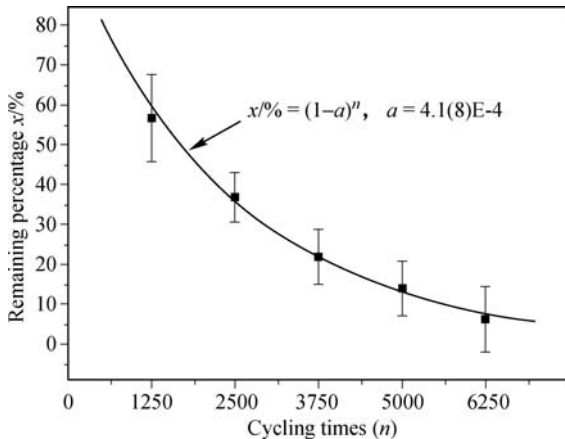
Fig. 4 The percentage of the remaining atoms in 6s5d $^3D_3$ against the number of 6s5d $^3D_3$–5d6p $^3F_4$ transition cycles. Setting the leakage rate a as the fitting parameter, we get the curve of exponential fitting. Corresponding to the function $x/\% = (1-a)^n$, a is determined to be 4.1(8)E-4.

Apart from the random measuring error which mainly

came from the drifting of the laser frequency and power and the fluctuation of the intensity of atomic beam, the simplification of the energy level structure model would also make systematic errors. Taking the lifetime of the lower state 6s5d $^3D_3$ into account, we found the corresponding uncertainty about a was 8E-10.

Since 5d6p $^3F_4$–5d^2 $^3F_{3,4}$ is the only permitted leakage channel of the 6s5d $^3D_3$–5d6p $^3F_4$ transition, the leakage rate is the ratio between the transition probabilities of 5d6p $^3F_4$–5d^2 $^3F_{3,4}$ and 5d6p $^3F_4$–6s5d $^3D_3$. Using Garcia's data, the sum of the probabilities of 5d6p $^3F_4$–5d^2 $^3F_3$ and 5d6p $^3F_4$–5d^2 $^3F_4$ was determined to be $2.1(4)\times10^4$ s^{-1}.

3 Calculation with scaled Thomas–Fermi–Dirac method

We also calculated the transition probabilities of all the seven lines between 6p5d ^3F and 5d^2 ^3F states as reference. The line strength is

$$\begin{aligned} S &= \langle\,[(L_c, l)L, S]\,J\,||P||\,[(L_c, l')L', S]\,J'\rangle \\ &= D_{\text{line}}^2 D_{\text{mult}}^2 P_{nl,n'l'}^2 \end{aligned} \tag{3}$$

in which

$$D_{\text{line}} = (-1)^{(L+S+J'+1)}[J, J']^{1/2} \left\{ \begin{matrix} L & S & J \\ J' & 1 & L' \end{matrix} \right\} \tag{4}$$

where

$$[J, J'] = (2J + 1)(2J' + 1) \tag{5}$$

And for the situation $l^w - l^{w-1}l'$, the active atom whose n and l quantum number are identical with other atoms in the initial or final configurations.

$$\begin{aligned} D_{mult} &= \sqrt{w}\langle l^n v_c SL\{|l^{n-1}v_c S_c L_c\rangle \\ &\cdot (-1)^{L_c+L+l'+1}[L, L']^{1/2} \left\{ \begin{matrix} l_c & l & L \\ 1 & L' & l' \end{matrix} \right\} \end{aligned} \tag{6}$$

$\langle l^n v_c SL\{|l^{n-1}v_c S_c L_c\rangle$ is the coefficient of fractional parentage [6], which has value 1 for the configuration of double electrons,

$$\begin{aligned} P_{nl,n'l'} &= \langle nl||r||n'l'\rangle \\ &= (-1)^l[l, l']^{1/2} \left(\begin{matrix} l & 1 & l' \\ 0 & 0 & 0 \end{matrix} \right) \int_0^\infty R_{nl} r R_{n'l'} \mathrm{d}r \end{aligned} \tag{7}$$

The radial wave function R_{nl} was calculated by the scaled Thomas–Fermi–Dirac method [5]. In the radial Schrödinger equation,

$$\left[-\frac{\mathrm{d}^2}{\mathrm{d}r^2} + \frac{l(l + 1)}{r^2} + V(r) \right] R(r) = ER(r) \tag{8}$$

$V(r)$ was written by Latter [7] as an approximative conditional function without the radial wave function,

$$V(r) = \min\left(V_{\text{TFD}}, -\frac{2}{r}\right) \tag{9}$$

$$V_{\text{TFD}}(r) = -\left[\frac{Z \cdot \varphi(r/\mu)}{r} + \frac{3\sqrt{2Z \cdot \varphi(r/\mu)}}{4\pi\sqrt{r}}\right] \tag{10}$$

in which $\mu = 0.8853Z^{-1/3}$ and Z is the atomic number. φ is the TF function, which was fitted by Latter as

$$\begin{aligned}
\varphi(\mu/r) = [&1 + 0.02747(\mu/r)^{1/2} + 1.243(\mu/r)\\
&- 0.1468(\mu/r)^{3/2} + 0.02747(\mu/r)^2\\
&+ 0.02747(\mu/r)^{5/2} + 0.02747(\mu/r)^3]^{-1} \tag{11}
\end{aligned}$$

Eq. (8) was solved by the numerical integration using the method of Numerov [8]. The result was plugged into Eq. (7), and finally the line strength $\mathcal{S}$ could be evaluated. Using the relation between the transition probability A and $\mathcal{S}$,

$$\begin{aligned}
A_{ki} &= \frac{1}{6}\left(\frac{e^2}{\hbar c}\right)^4 \frac{c}{a_0 g_k}\left(\frac{|T_i - T_k|}{R_\infty}\right)^3 \frac{S}{e^2 a_0^2}\\
&= \frac{2.0261 \times 10^{18}}{g_k \lambda^3} \tag{12}
\end{aligned}$$

the transition probabilities were determined. a_0 is the Bohr radius, T_i, T_k, g_k are the term values and the statistical weight of the upper and the lower levels, and R_∞ is the Rydberg constant. The final results are listed in Table 1, along with the three transition lines previously calculated by Kulaga *et al.* [9] making use of the "Hartree–Fock with relativistic corrections (HFR) method". The other four are completely new results. The transition probabilities of 5d6p $^3F_4$–5d^2 $^3F_3$ and 5d6p $^3F_4$–5d^2 $^3F_4$ were determined to be 4.8×10^3 s^{-1} and 4.5×10^4 s^{-1} respectively. The difference from the experimental data is probably due to configuration mixing.

Table 1 The calculation result of 6p5d ^{3}F–5d^2 ^{3}F transition.

Upper levels	Lower levels	Wavelength/Å	Results of STFD	Previous work [9]
5d6p $^3F_2$	5d^2 $^3F_2$	88447.8	6.3×10^3	$(4.4{\sim}6.4) \times 10^3$
	5d^2 $^3F_3$	122782.2	3.0×10^2	–
5d6p $^3F_3$	5d^2 $^3F_2$	49667.5	3.2×10^3	$(4.48{\sim}6.55) \times 10^3$
	5d^2 $^3F_3$	58919.6	2.0×10^4	$(2.99{\sim}4.43) \times 10^4$
	5d^2 $^3F_4$	75548.7	9.2×10^2	–
5d6p $^3F_4$	5d^2 $^3F_3$	39890.6	4.8×10^3	–
	5d^2 $^3F_4$	46876.2	4.5×10^4	–

4 Conclusions

Both experimental measurement and theoretical calculation were used to determine the transition probabilities of 5d6p ^{3}F–5d^2 ^{3}F for barium. As far as we know, no experiment has been performed on this transition series and only 3 of 7 lines have been calculated. These new data are very important in searching for a more convenient and effective laser cooling method of barium atoms on metastable D state. According to these data, it should be a little difficult to achieve the laser cooling of barium directly with a single 706 nm laser. To overcome the leakage to the 5d^2 ^{3}F states, some repumping method should be found. Otherwise, another scheme choosing the state 5d6p $^3F_2$ as the upper level may be taken into account, because the transition probability from 5d6p $^3F_2$ to ^{3}F–5d^2 ^{3}F is about one order lower than that of 5d6p $^3F_4$.

References

1. M. M. Boyd, A. D. Ludlow, S. Blatt, S. M. Foreman, T. Ido, T. Zelevinsky, and J. Ye, Phys. Rev. Lett., 2007, 98(8): 083002

2. S. De, U. Dammalapati, K. Jungmann, and L. Willmann, Phys. Rev. A, 2009, 79(4): 041402(R)

3. J. Migdalek and W. E. Baylis, Phys. Rev. A, 1990, 42(11): 6897

4. G. Garcia and J. Campos, J. Quant. Spectrosc. Radiat. Transf., 1989, 42(6): 567

5. J. C. Stewart and M. Rotenberg, Phys. Rev. A, 1965, 140(5): A1508

6. G. K. Oertel and L. P. Shomo, Astrophys. J. Suppl. Ser., 1968, 16: 175

7. R. Latter, Phys. Rev., 1955, 99(2): 510

8. B. Numerov, Publ. Observ. Central Astrophys. Russ., 1933, 2: 188

9. D. Kulaga, J. Migdalek, and O. Bar, J. Phys. B: Mol. Opt. Phys., 2001, 34(23): 4775